Original Paper

High-temperature spectroscopic study of redox reactions in iron- and arsenic-doped melts

Henning Schirmer, Matthias Müller and Christian Rüssel

Otto-Schott-Institut für Glaschemie, Friedrich-Schiller-Universität Jena, Jena (Germany)

Glasses with the basic composition $16Na_2O \cdot 10CaO \cdot 74SiO_2$ doped with iron or with both iron and arsenic were studied by means of high-temperature UV-VIS-NIR spectroscopy. Increasing temperatures led to a shift of the UV absorption edge caused by Fe^{3+}-charge transfer bands to larger wavelengths. All other bands, especially the Fe^{2+} absorption band at around 1100 nm, decreased in intensity at higher temperatures. For glasses, solely doped with iron, the temperature dependency of the extinction coefficient was quantitatively determined. Glasses doped with both arsenic and iron showed a different behaviour: the intensity of the bands decreased up to a temperature of 600 to 650 °C and then increased again. This can be explained by the temperature-dependent redox reaction $2Fe^{3+} + As^{3+} \rightleftharpoons 2Fe^{2+} + As^{5+}$. Increasing temperatures lead to a shift of the reaction to the right. This reaction is in equilibrium at temperatures > 650 °C and gets frozen in at smaller temperatures, depending on the respective iron and arsenic concentrations. The latter is explained by a numerical simulation assuming the redox reactions to be controlled by diffusion.

1. Introduction

Transition elements in glasses occur in different oxidation states. The physical properties of the glasses are strongly affected not only by the type and concentration, but also by the redox state of these transition elements. At temperatures far above the glass transition temperature, polyvalent elements are in equilibrium with the physically dissolved oxygen in the melt [1 to 4]

$$A^{(n-z)+} + \frac{z}{4} O_2 \xrightleftharpoons{K_A(T)} A^{n+} + \frac{z}{2} O^{2-} . \quad (1)$$

The equilibrium constant K'_A can be defined as follows:

$$K'_A(T) = \frac{a_{A^{n+}} \cdot a_{O^{2-}}^{z/2}}{a_{A^{(n-z)+}} \cdot a_{O_2}^{z/4}} \quad (2)$$

with a = activities of the respective species.

Since $a_{O^{2-}}$ is usually much larger than the concentrations of the polyvalent elements, it can be incorporated into the equilibrium constant ($K_A(T)$). Furthermore, the ratios $[A^{n+}]/[A^{(n-z)+}]$ as determined in the cooled glass do not depend upon the total concentration of the polyvalent ion in the cooled glass within the limits of error for concentration < 1 mol%. Hence, in good approximation, activity coefficients of the polyvalent element can be considered to be unity (if referenced to ideally diluted solutions) and the activities in equation (2) replaced by the concentrations [3 and 5].

Received 5 June 2002, revised manuscript 21 December 2003.

$$K_A(T) = \frac{[A^{n+}]}{[A^{(n-z)+}]} \frac{1}{a_{O_2}^{z/4}} . \quad (3)$$

Redox equilibria in glass melts are generally shifted to the oxidized species during cooling and hence the oxygen activity decreases. If only one polyvalent element occurs, the ratio $[A^{n+}]/[A^{(n-z)+}]$ remains constant during rapid cooling if the concentration of the reduced species is much larger than that of physically dissolved oxygen [1, 2 and 6]. In technical glass melts, this is usually the case. Since the diffusion of oxygen from the atmosphere into the melt is a fairly slow process, the $[A^{n+}]/[A^{(n-z)+}]$ ratio remains constant, while cooling a technical silicate melt using rates convenient in the technical process.

If, however, more than one polyvalent element is present, this situation changes and redox reactions during cooling may play an important part. In the literature, some studies have been reported in which a melt containing two types of polyvalent elements has been equilibrated with an atmosphere of well defined oxygen activity and subsequently been cooled [7 to 10]. Here, a clear deviation of the redox ratio $[A^{n+}]/[A^{(n-z)+}]$ from that of a melt solely doped with the polyvalent element A has been found. Since at the temperature of equilibration, the redox ratio $[A^{n+}]/[A^{(n-z)+}]$ should not be affected by the presence of another type of polyvalent element [4, 11 and 12] (at small concentrations and the same atmosphere), this is also a hint that redox reactions took place during cooling. A priori, however, a mutual interaction between different polyvalent elements also at high temperatures should not be excluded [7]. High-temperature spectroscopic studies which allow to monitor these redox reactions and also to conclude on (possible) freezing-in tem-

peratures have scarcely been carried out; only two studies have been reported using high-temperature EPR spectroscopy [11 and 12]. This paper provides a study on redox reactions in melts doped with both As_2O_5 and Fe_2O_3 by means of UV-VIS-NIR spectroscopy, including a theoretical description of the results obtained.

2. Theory

If a glass melt contains a second polyvalent ion B, by analogy to equation (2), an equilibrium constant K_B can be defined:

$$B^{(m-y)+} + \frac{y}{4} O_2 \xrightleftharpoons{K_B(T)} B^{m+} + \frac{y}{2} O^{2-} , \tag{4}$$

$$K_B(T) = \frac{[B^{m+}]}{[B^{(m-y)+}]} \frac{1}{a_{O_2}^{y/4}} . \tag{5}$$

The equilibrium constants K_A and K_B depend upon temperature

$$-RT \ln K_A = \Delta G_A^0 = \Delta H_A^0 - T\Delta S_A^0 , \tag{6}$$

$$-RT \ln K_B = \Delta G_B^0 = \Delta H_B^0 - T\Delta S_B^0 . \tag{7}$$

In presence of the two polyvalent elements A and B, the redox reaction (8) may take place if the temperature is changed [4].

$$zB^{(m-y)+} + yA^{n+} \xrightleftharpoons{K_{AB}(T)} zB^{m+} + yA^{(n-z)+} . \tag{8}$$

The temperature dependence of the equilibrium constant K_{AB} is given by the temperature dependences of equations (1 and 4). Thus from equations (6 and 7), it follows:

$$\begin{aligned} K_{AB}(T) = \frac{K_A^y(T)}{K_B^z(T)} &= \exp[(-y\Delta G_A^0 + z\Delta G_B^0)/(RT)] \\ &= \exp[(z\Delta H_B^0 - y\Delta H_A^0)/(RT)] \\ &\cdot \exp[(y\Delta S_A^0 - z\Delta S_B^0)/(RT)] . \end{aligned} \tag{9}$$

Thus, the equilibrium according to equation (8), will usually depend on temperature (if $\Delta H_A^0 \neq \Delta H_B^0$). Hence, if the temperature changes, also the redox ratios $[A^{n+}]/[A^{(n-z)+}]$ and $[B^{(m-y)+}]/[B^{m+}]$ will change because here oxygen diffusion in or out of the melt is not necessary. It should be noted that this is in contrast to melts containing only one polyvalent element.

Up to now, solely the thermodynamics is considered. However, it is well known that at high temperatures the melts are in equilibrium, but it should be assumed that below a certain temperature, the equilibrium should be frozen in. Kinetics of a redox reaction according to equation (8) can be described by the rate constants k_+ and k_- of the forward and backward reactions, respectively.

$$zB^{(m-y)+} + yA^{n+} \underset{k_-}{\overset{k_+}{\rightleftharpoons}} zB^{m+} + yA^{(n-z)+} . \tag{10}$$

Assuming electron transfer reactions to be much faster than the diffusion, the rate constants are diffusion-controlled and

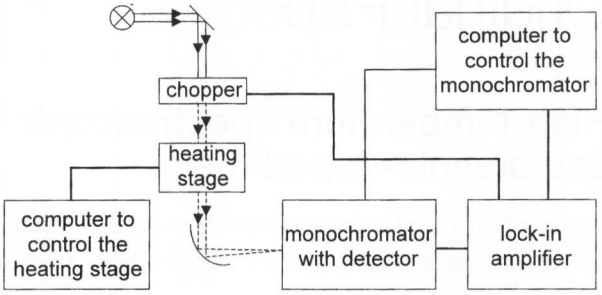

Figure 1. Schematic drawing of the experimental arrangement used for high-temperature UV-VIS-NIR spectroscopy.

can be estimated only for a bimolecular reaction by the Smoluchowsky equation.

$$k = C_0(D_A + D_B)(r_A + r_B) \tag{11}$$

with $C_0 = 7.57 \times 10^{24}\ mol^{-1}$, D_A, D_B the diffusion coefficients, and r_A, r_B the ionic radii of the respective species.

In this paper, a bimolecular reaction cannot be assumed (since $z = 2$, $y = 1$ in equation (10)) and equation (11) cannot be applied. In the discussion, however, it was assumed (by analogy to equation (11)) that the rate constants of equation (10) are also proportional to the diffusivities.

3. Experimental

Glasses with the basic composition (in mol%) 74 SiO_2 · 16 Na_2O · 10 CaO doped with As_2O_3 and Fe_2O_3 were melted from reagent-grade raw materials Na_2CO_3, $CaCO_3$, Fe_2O_3, $Fe(C_2O_4)$ · 2 H_2O and As_2O_3 in a high-frequency furnace in a platinum crucible (200 ml) using a maximum temperature of 1500 °C. The glasses were doped with 0.5 mol% Fe (sample A), 0.5 mol% Fe + 0.25 mol% As (sample B), 1 mol% Fe + 0.5 mol% As (sample C) and 1 mol% Fe + 1 mol% As (sample D). For samples A to D, Fe_2O_3 was used as raw material, additionally, a sample with 0.5 mol% Fe was melted using $Fe(C_2O_4)$ · 2 H_2O as raw material (sample E). The glasses were cast on a graphite mould, preheated to 600 °C and subsequently cooled applying a cooling rate of 30 K/h.

Spectra at room temperature were collected in the wave number range of 3000 to 30 000 cm^{-1}. High-temperature absorption spectra were recorded in the temperature range from 25 to 750 °C using a halogen lamp as light source. The light was reflected by a planar mirror, passed a chopper (frequency 113 s^{-1}) and subsequently the sample. The transmitted light was reflected by 90° by an off-axis parabolic mirror (focal distance: 45 cm) and focused to the entrance slit of a monochromator TRIAX 320 (Jobin – Yvon, Edison, NY (USA)). The sample was placed in a heating chamber of a microscope heating stage (TS 1500 LINCAM, Waterfield (UK)). An Si-detector as well as a PbS-detector were used, the signals were given to a lock-in amplifier SR 830 (Stanford Research Systems, Stanford (USA)), adjusted to the chopper frequency. All the samples had a diameter of 6 mm and were 2.0 mm thick. The surfaces were ground and polished. The experimental arrangement is shown in figure 1.

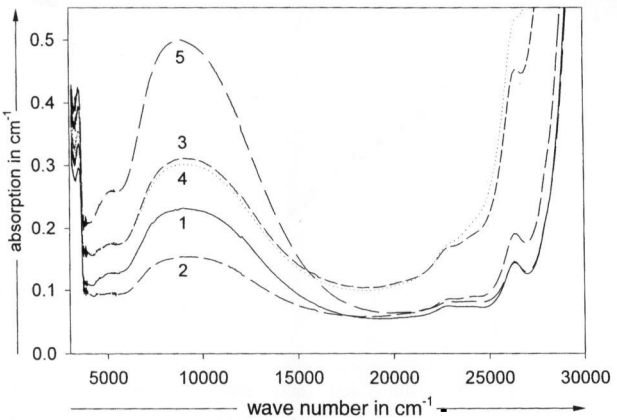

Figure 2. Absorption spectra recorded at room temperature. curve 1: sample A, curve 2: sample B, curve 3: sample C, curve 4: sample D, curve 5: sample E.

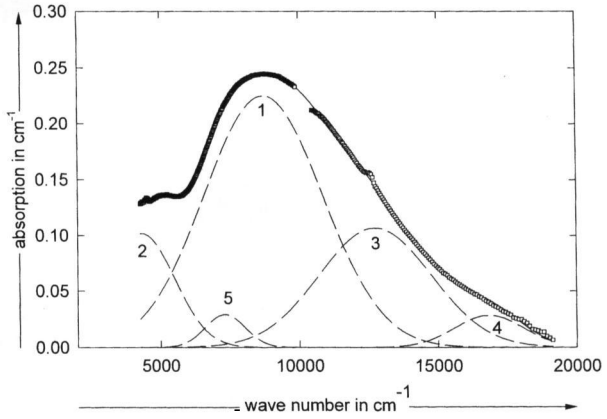

Figure 3. Absorption spectrum recorded at room temperature (squares); dashed curves: deconvoluted absorption peaks of Gaussian shape, full line: sum of the dashed curves.

4. Results

In figure 2, absorption spectra of the samples recorded at room temperature are shown. The spectra show distinct absorptions at around 5500, 9000, 23 000 and 27 000 cm^{-1}. According to [9, 10 and 13], the first two absorption bands are caused by Fe^{2+}, while the latter two are due to Fe^{3+}. The largest Fe^{2+} absorptions are observed in the sample melted using $Fe(C_2O_4) \cdot 2\,H_2O$ as raw material (see curve 5). The absorption at 9000 cm^{-1} is much smaller in the sample prepared from Fe_2O_3 (see curve 1) and smallest in the sample doped with Fe_2O_3 and As_2O_3 (see curve 2). These curves (1, 2 and 5) are attributed to 0.5 mol% Fe, while curves 3 and 4 are both recorded from glasses containing 1 mol% Fe. The absorptions caused by both Fe^{2+} and Fe^{3+} are larger than those in samples 1 and 2. Figure 3 shows a spectrum of sample A recorded using the high-temperature equipment shown in figure 1. The spectrum was recorded at room temperature and then deconvoluted using five distinct absorption bands. The bands at 4000 and 9000 cm^{-1} are attributed to the Fe^{2+} with an octahedral symmetry (O_h) and a transition of $^5\Gamma_5$ (D) $\rightarrow$ $^5\Gamma_3$ (D) and Fe^{2+} with a tetrahedral symmetry (T_α) and a transition of $^5\Gamma_3$ (D) $\rightarrow$ $^5\Gamma_5$ (D) [9, 10 and 13]. The bands at 13 000 and 17 000 cm^{-1} according to [9, 10 and 13] are caused by the Fe^{3+} (O_h) $^6\Gamma_1$ (s) $\rightarrow$ $^4\Gamma_5$ (G) transitions. An attribution of band 5 is not given in the literature, although the occurrence has already been described. As shown in figure 3, the experimental spectrum (see squares) is in good agreement with the superposition of the bands 1 to 5.

Figure 4 shows absorption spectra of sample A recorded at temperatures in the range of 25 to 750 °C. While curve 1 (25 °C) shows a distinct peak at around 380 nm attributed to the Fe^{3+} $^6\Gamma_1(s)$ $\rightarrow$ $^4\Gamma_5$ (D) transition, this peak is not visible at higher temperatures. The UV absorption edge caused by charge transfer transitions is continuously shifted to larger wavelengths as already reported in the literature [14] and due to its much higher intensity covers the band at 380 nm. Hence, this line cannot be used to detect the Fe^{3+} concentration at higher temperatures. Figure 5 shows the absorption spectra for higher temperatures. The absorption band at 1100 nm due to Fe^{2+} decreases in intensity for higher temperatures and is slightly shifted to larger wavelengths. By analogy, the intensity of the band at 2000 nm which is also caused by Fe^{2+} decreases with increasing temperature. The decreasing intensity of the bands attributed to Fe^{2+} has already been reported in the literature (see e. g. [2]) and explained by a weakening of the ligand field. The bands at wavelengths larger than 2500 nm are caused by

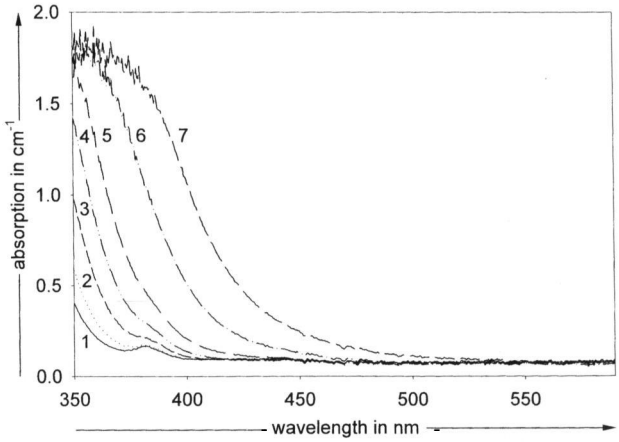

Figure 4. Absorption spectra of sample A for shorter wavelengths recorded in the temperature range of 25 to 750 °C; curve 1: 25 °C, curve 2: 100 °C, curve 3: 200 °C, curve 4: 300 °C, curve 5: 400 °C, curve 6: 600 °C and curve 7: 750 °C.

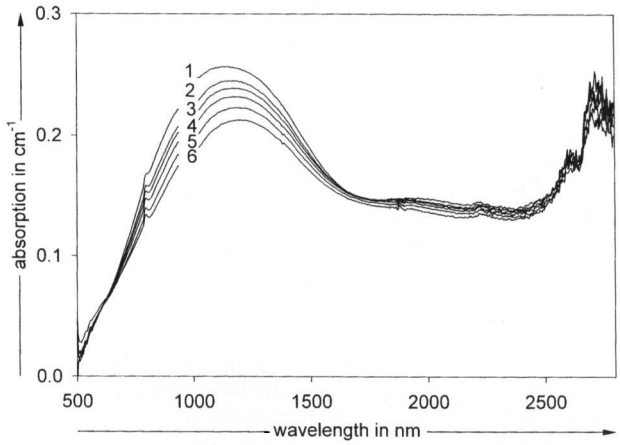

Figure 5. Absorption spectra of sample A for larger wavelengths recorded in the temperature range of 25 to 750 °C; curve 1: 25 °C, curve 2: 300 °C, curve 3: 400 °C, curve 4: 500 °C, curve 5: 600 °C and curve 6: 750 °C.

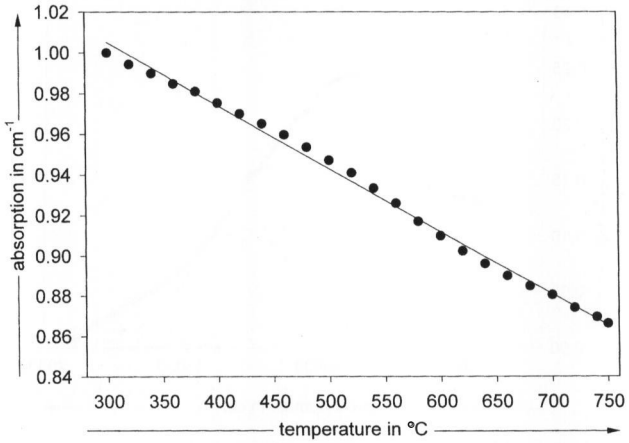

Figure 6. Absorption at the maximum of the band at around 1100 nm as a function of temperature for sample A. The absorptions are normalized to 300 °C.

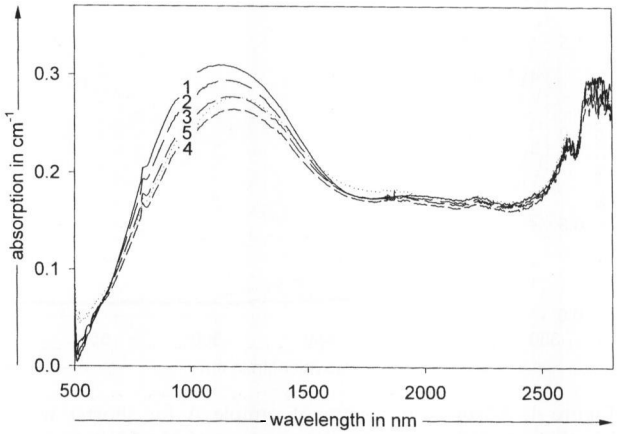

Figure 7. Absorption spectra of sample C recorded in the temperature range of 25 to 750 °C; curve 1: 25 °C, curve 2: 300 °C, curve 3: 500 °C, curve 4: 600 °C and curve 5: 750 °C.

water and will not be discussed in the following. Figure 6 shows the absorption of the maximum of the band at around 1100 nm as a function of the temperature. The absorptions are normalized to 300 °C. A steady, and within the limits of error linear decrease is observed in the temperature range of 300 to 750 °C. In figure 7, the absorption spectra of sample C are shown as a function of the temperature. This glass contains 1 mol% Fe and additionally 0.5 mol% As. First, a fairly similar behaviour as in figure 5 is observed, the intensity of the bands at around 1100 and 2000 nm decreases while increasing the temperature from 25 to 600 °C. However, the curve recorded at 750 °C clearly shows larger absorptions at both 1100 and 2000 nm than that recorded at 600 °C. In figures 8a to c, the absorptions normalized to 300 °C are shown as a function of the temperature for the samples B, C and D, respectively. At first glance, all curves show the same behaviour: up to a temperature of around 575 °C, the absorption decreases linearly (within the limits of error) and then increases again while further increasing the temperature. In more detail, the temperature at which a first deviation from linearity is observed depends on the glass studied: these temperatures are 640, 620 and 600 °C for the samples B, C and D, respectively.

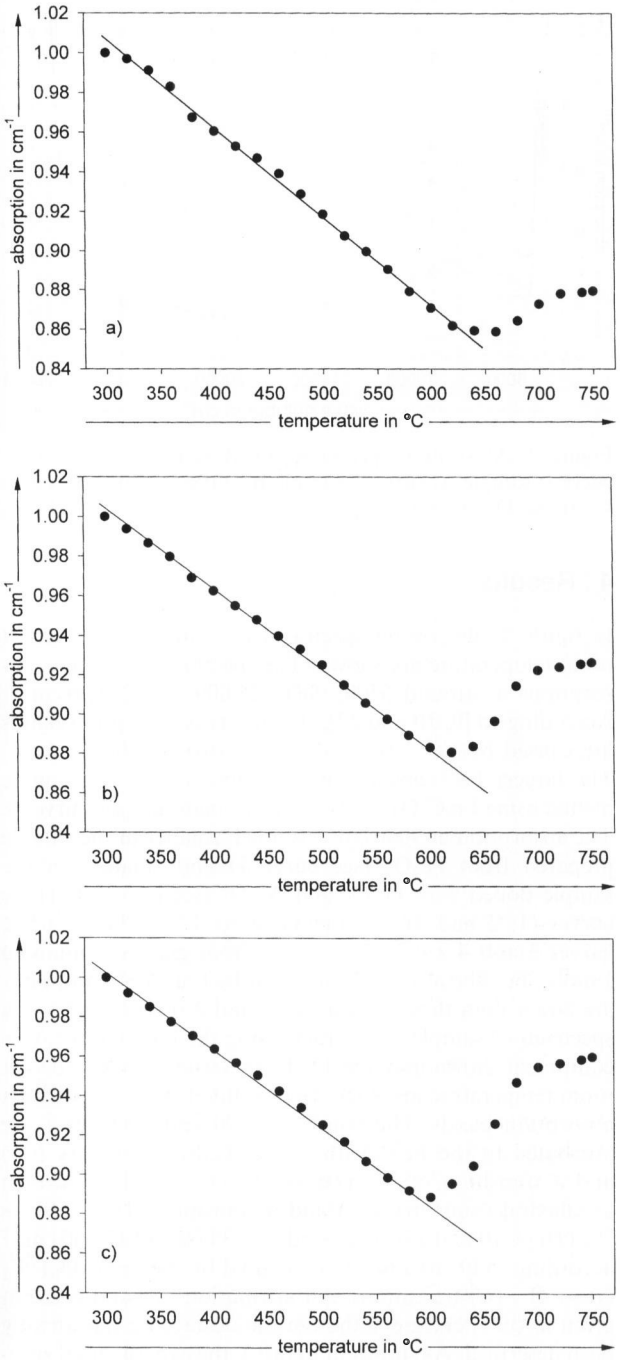

Figures 8a to c. Absorption at the maximum of the band at around 1100 nm as a function of the temperature. The absorptions are normalized to 300 °C. Figure a): sample B, figure b): sample C, and figure c): sample D.

5. Discussion

To study redox reactions in iron-containing glasses using high-temperature absorption spectroscopy, the wavelengths below 700 nm are less advantageous, because of the strong shift of the UV absorption range to larger wavelengths at higher temperatures. Distinct peaks attributed to Fe^{3+} are no longer visible at temperatures larger than 400 °C. However, the absorption peak at 1100 nm attributed to Fe^{2+} is suitable to quantitatively determine Fe^{2+} in the glass. In sample A containing iron as the only polyvalent element, a linear decrease in intensity with increasing temperature is

Table 1. Absorptions, Fe^{2+} and Fe^{3+} concentrations as well as redox ratios for different temperatures and samples A, B, C and D

temperature in °C	A	B	C	D
	absorption in arbitrary units			
600	0.910	0.87	0.879	0.882
650	0.893	0.858	0.888	0.912
700	0.881	0.871	0.92	0.952
750	0.866	0.878	0.924	0.958
	$[Fe^{2+}]$ in mol%			
600	0.097	0.057	0.110	0.098
650	0.097	0.0577	0.1137	0.1036
700	0.097	0.0602	0.1206	0.1107
750	0.097	0.06247	0.1242	0.1141
	$[Fe^{3+}]$ in mol%			
600	0.408	0.456	0.890	0.902
650	0.408	0.4553	0.8863	0.896
700	0.408	0.451	0.8793	0.8893
750	0.408	0.4505	0.8758	0.8859
	$[Fe^{2+}]/[Fe^{3+}]$ ratio			
600	0.238	0.125	0.1236	0.1086
650	0.238	0.127	0.1283	0.1156
700	0.238	0.133	0.1371	0.1245
750	0.238	0.139	0.1418	0.1288

observed. This decrease in intensity is only around 13 % in the range of 300 to 750 °C, and hence the absorption can clearly be monitored within the whole temperature range studied. Within this range, the absorption decreases in all glasses studied (samples A to E) to a value of 0.89 ± 0.017, regardless of the oxidation state (samples A and E), the total iron concentration or the additional occurrence of arsenic oxide. That means, the decrease in absorption with temperatures in all samples studied is the same and hence also in the case of samples additionally doped with arsenic, the Fe^{2+} concentration does not change during heating to temperatures of up to 600 °C. Thus, a redox reaction according to equation (4) does not take place. At temperatures larger than 600 °C, the behaviour of glasses containing additionally arsenic oxide differs from those solely containing iron. The absorptions and, thus, the concentrations of Fe^{2+} increase again while further increasing the temperature. In [15], extinction coefficients of Fe^{2+} and Fe^{3+} as well as of redox ratios in the glasses studied at room temperatures are reported. From these data, Fe^{2+} and Fe^{3+} as well as redox ratios were calculated and summarized in table 1. Since the Fe^{2+} concentration cannot change in the samples A and E while changing the temperature, the effect of temperature upon the extinction coefficient of Fe^{2+} can be taken from figure 6. This enables the calculation of Fe^{2+} concentrations of the samples B to D also at temperatures larger than 600 °C. The results are included in table 1.

The samples were melted under identical conditions, the maximum temperature applied was 1500 °C in any case. In the following, it is assumed that the melt was in equilibrium with the same oxygen fugacity as sample A at this temperature. From this starting point, the shift in the concentrations of the respective redox species was calculated. Figure 9

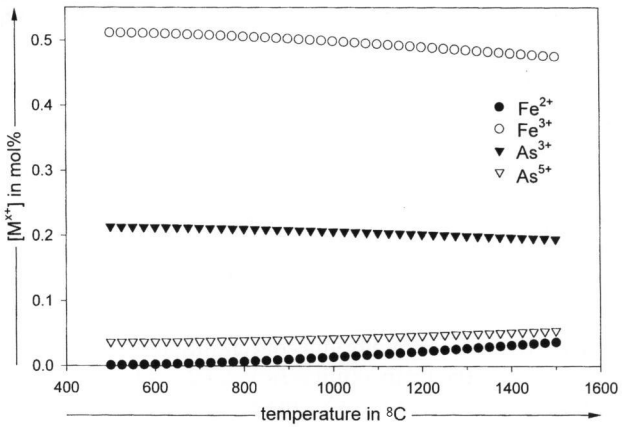

Figure 9. Concentrations of Fe^{2+}, Fe^{3+}, As^{3+} and As^{5+} as a function of the temperature in sample B for equilibrium conditions calculated by using voltammetrically determined ΔH^0 and ΔS^0 values of the respective redox reactions.

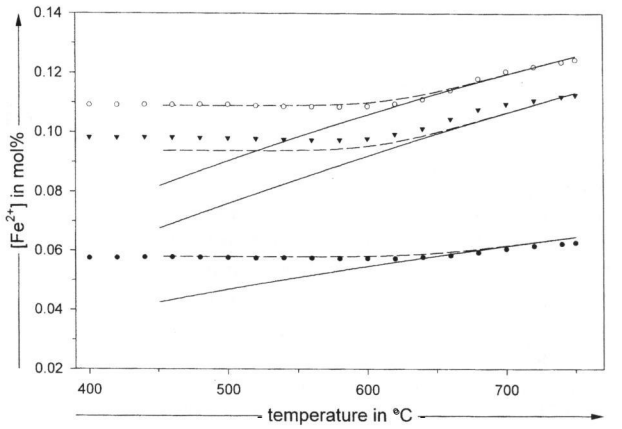

Figure 10. Concentrations of Fe^{2+} as a function of the temperature in arsenic oxide doped glasses obtained by numerical simulations of equation (14) (dashed lines). Equilibrium values (full lines). Experimentally determined Fe^{2+} concentrations from figures 8a to c; o: sample B, ▼: sample C, and •: sample D.

shows these calculations using thermodynamic values (As^{3+}/As^{5+}: $\Delta H^0 = 230$ kJ mol^{-1}, $\Delta S^0 = 138$ J K^{-1} mol^{-1}, Fe^{2+}/Fe^{3+}: $\Delta H^0 = 102$ kJ mol^{-1}, $\Delta S^0 = 33$ J K^{-1} mol^{-1}) measured voltammetrically in the temperature range from 1000 to 1300 °C. The curve shows that the concentration of Fe^{2+} decreases with decreasing temperature for all sample compositions. This is also observed in the experiments: sample B should possess the same $[Fe^{2+}]/[Fe^{3+}]$ ratio at 1500 °C as sample A (0.238); during cooling the ratio decreases until a value of 0.125 is reached at room temperature. The Fe^{2+} concentrations calculated, however, are smaller than those observed experimentally. It should be noted that the thermodynamic values (ΔH^0, ΔS^0) were obtained at much larger temperatures and especially the extrapolation to temperatures near T_g is doubtful. In figure 10 (full lines), the thermodynamic values of ΔH^0 for both redox pairs were altered ($\Delta H^0_A - \Delta H^0_B = 231$ kJ mol^{-1} (see equation (9)) in order to obtain maximum agreement of experimental values with those calculated. For temperatures > 650 °C, the thermodynamic data set fits the values obtained for all samples measured. It should be noted that also the comparatively small Fe^{2+} concentration of sample D (here the Fe^{2+}/Fe^{3+} value is smaller than in the samples

B and D) is explained for temperatures in the range of around 600 to 750 °C.

The kinetics of the redox reaction shown in equation (8) can be described by a differential equation, assuming a trimolecular reaction:

$$\frac{dx}{dt} = ([Fe^{2+}]_0 - x)^2\,([As^{5+}]_0 - x/2)\,k_+ - ([Fe^{3+}]_0 + x)^2\,([As^{3+}]_0 + x/2)\,k_- \quad (12)$$

with $[A^z]_0$ = initial equilibrium concentration of the respective species; at the temperatures T_0 x, $x / 2$ = changes in the respective concentrations with time.

In the following, a constant cooling rate, $1/r$, was assumed which was applied to the respective melt samples. The attributed temperature is $T = T_0 - t/r$, with T_0 = initial temperature ($dx/dt = -r\,dx/dT$). It follows:

$$-\frac{dx}{dT} = \{([Fe^{2+}]_0 - x)^2\,([As^{5+}]_0 - x/2)\,k_+ - ([Fe^{3+}]_0 + x)^2\,([As^{3+}]_0 + x/2)\,k_-\}\,\frac{1}{-r}. \quad (13)$$

The ratio of the rate constants k_+ and k_- is equal to the equilibrium constant K_{AB}. Furthermore, according to [4], the reaction was assumed to be controlled by diffusion. Although, as already mentioned, k_+ cannot be calculated by equation (11), the activation energy of the rate constant k_+ should have the same value as that of the diffusion coefficient of iron (330 kJ mol^{-1}) [16]. This seems to be justified since arsenic diffusion coefficients are much smaller than those of iron [16]. From equation (13), it follows with $k_+ = C\,exp(E_D/(R\,T))$, C = constant, and E_D = 330 kJ mol^{-1}:

$$-\frac{dx}{dT} = \{([Fe^{2+}]_0 - x)^2\,([As^{5+}]_0 - x/2) - ([Fe^{3+}]_0 + x)^2\,([As^{3+}]_0 + x/2)\,K_{AB}\,(T)\} \quad (14)$$
$$C/r \exp\,(E_D/(R\,T))\,.$$

Equation (14) cannot be solved analytically, however, a numerical solution is easily possible. In the following, the thermodynamic data already used for the calculation of figure 9 were taken. Figure 10 shows numerical simulations of equation (14) for $C/r = 4.85 \times 10^{18}$ mol%$^{-2}$ K^{-1}. Starting from 1500 °C, the temperature was continuously decreased. The resulting Fe^{2+} concentrations up to a temperature of around 660 °C are identical with the equilibrium concentrations. At temperatures below 620 °C, the Fe^{2+} concentrations remain constant. The redox freezing-in temperature is defined as that temperature, the equilibrium redox concentrations are equal to those of the cooled glass. Since the cooling rates as well as the constant C are not known, the value of C/r (4.85×10^{18} mol%$^{-2}$ K^{-1}) was fitted to obtain a freezing-in temperature (645 °C) equal to that of sample B. The values for the samples C and D were obtained using the same data set, including C/r. It is seen that the freezing-in temperatures decrease with increasing concentrations. In sample C and D, freezing-in temperatures of 624 and 613 °C were calculated, which is in agreement with the experimentally determined values.

6. Conclusions

For the first time, the occurrence of redox reactions between polyvalent elements during cooling of a melt was proved using high-temperature UV-VIS-NIR spectroscopy. During cooling of a melt containing both iron and arsenic oxide, a redox reaction takes place. The equilibrium $2Fe^{3+} + As^{3+} \rightleftharpoons 2Fe^{2+} + As^{5+}$ is shifted to the right. At temperatures >650 °C, the redox reaction is in equilibrium and gets frozen-in at lower temperatures. The larger the iron and arsenic concentrations, the lower the freezing-in temperature. The thermodynamic behaviour can qualitatively be explained by calculating the concentration of the redox species from thermodynamic data ΔH^0 and ΔS^0 measured voltammetrically at high temperatures. The freezing-in of the redox reaction can be explained by numerical simulations of the respective differential equation assuming the redox reaction to be controlled by diffusion.

*

Thanks are due to the Deutsche Forschungsgemeinschaft (DFG), Bonn-Bad Godesberg, for financial support.

7. References

[1] Paul, A.: Effects of thermal stabilization on the redox equilibria and colour of glass. J. Non-Cryst. Solids **71** (1985) pp. 269–278.

[2] Schreiber, H. D.; Hockman, A. L.: Redox chemistry in candidate glasses for nuclear waste immobilization. J. Am. Ceram. Soc. **70** (1987) pp. C 106–C 108.

[3] Rüssel, C.: Iron oxide-doped alkali-lime-silica glasses. Pt. 2. Voltammetric studies. Glastech. Ber. **66** (1993) pp. 93–99.

[4] Rüssel, C.: Redox reactions during cooling of glass melts – a theoretical consideration. Glastech. Ber. **62** (1989) pp. 199–203.

[5] Gerlach, S.; Claußen, O.; Rüssel, C.: Thermodynamics of iron in alkali-magnesia-silica glasses. J. Non-Cryst. Solids **238** (1998) pp. 75–82.

[6] Rüssel, C.; Kohl, R.; Schaeffer, H. A.: Interaction between oxygen activity of Fe_2O_3 doped soda-lime-silica glass melts and physically dissolved oxygen. Glastech. Ber. **61** (1988) pp. 209–213.

[7] Xiang, Z. D.; Cable, M.: Redox interactions between Cu and Se, Sn, As, Sb in a soda-lime-silica glass. Phys. Chem. Glasses **38** (1997) pp. 167–172.

[8] Paul, A.; Douglas, R. W. : Mutual interaction of different redox pairs in glass. Phys. Chem. Glasses **7** (1966) pp. 1–13.

[9] Schreiber, H. D.; Minnix, L. M.; Carpenter, B. E. et al.: The chemistry of uranium in borosilicate glasses, Pt. 3. Mutual interactions of oxidising agents (Ce^{4+}, Cr^{6+}, Fe^{3+} and Mn^{3+}) with uranium in a base composition relevant to the immobilisation of nuclear waste. Phys. Chem. Glasses **24** (1983) pp. 155–165.

[10] Müller-Simon, H.: Electron exchange reactions between polyvalent elements in soda-lime-silica and sodium borate glasses. Glastech. Ber. Glass Sci. Technol. **69** (1996) pp. 387–395.

[11] Gravanis, G.; Rüssel, C.: Redox reactions in Fe_2O_3, As_2O_3 and Mn_2O_3 doped soda-lime-silica glasses during cooling – a high-temperature ESR – investigation. Glastech. Ber. **62** (1989) pp. 345–350.

[12] Gödeke, D.; Müller, M.; Rüssel, C.: High-temperature UV-VIS-NIR spectroscopy of chromium-doped glasses. Glastech. Ber. Glass. Sci. Technol. **74** (2001) pp. 177–182).

[13] Traverse, J.-P.; Toganidis, T.; Adès, C.: Spectrophotometric analysis of ferrous, ferric and total iron content in soda-lime-silica glass. Glastech. Ber. **65** (1992) pp. 201–206.
[14] Adès, C.; Toganidis, T.; Traverse, J.-P. : High temperature optical spectra of soda-lime-silica glasses and modelization in view of energetic applications. J. Non-Cryst. Solids **125** (1990) pp. 272–279.
[15] Bamford, C. R.; Hudson, E. J.: A spectrophotometric method for the determination of ferrous/ferric ratio of iron in soda-lime-silica glass. In: Proc. VIIe Congrès Internationales du Verre, Brussels 1965. Vol. I, pp. 6.1–6.11.
[16] Rüssel, C.: Self diffusion of polyvalent ions in a soda-lime-silica glass melt. J. Non-Cryst. Solids **134** (1991) pp. 169–175.

E203P001

Contact:

Prof. Dr. C. Rüssel
Otto-Schott-Institut für Glaschemie
Friedrich-Schiller-Universität Jena
Fraunhoferstraße 6
D-07743 Jena

E-mail: ccr@rz.uni-jena.de